

# CrystEngComm

Accepted Manuscript



This is an *Accepted Manuscript*, which has been through the Royal Society of Chemistry peer review process and has been accepted for publication.

*Accepted Manuscripts* are published online shortly after acceptance, before technical editing, formatting and proof reading. Using this free service, authors can make their results available to the community, in citable form, before we publish the edited article. We will replace this *Accepted Manuscript* with the edited and formatted *Advance Article* as soon as it is available.

You can find more information about *Accepted Manuscripts* in the [Information for Authors](#).

Please note that technical editing may introduce minor changes to the text and/or graphics, which may alter content. The journal's standard [Terms & Conditions](#) and the [Ethical guidelines](#) still apply. In no event shall the Royal Society of Chemistry be held responsible for any errors or omissions in this *Accepted Manuscript* or any consequences arising from the use of any information it contains.



## Uniform Decoration of Pt Nanoparticles on Well-Defined CdSe Tetrapods and Their Effect of Pt Cluster Size on the Photocatalytic H<sub>2</sub> Generation

Received 00th January 20xx,  
Accepted 00th January 20xx

DOI: 10.1039/x0xx00000x

www.rsc.org/

Younghun Sung,<sup>ab</sup> Jaehoon Lim,<sup>d</sup> Jai Hyun Koh,<sup>e</sup> Lawrence J. Hill,<sup>c</sup> Byoung Koun Min,<sup>e</sup> Jeffrey Pyun<sup>bc\*</sup> and Kookheon Char<sup>ab\*</sup>

**Colloidal metal-semiconductor hybrid nanocrystals are of great interest due to the synergistic effect originating from multifunctionalities within a single nanocrystal for various applications. Among them, platinum-incorporated cadmium chalcogenide hybrid nanocrystals have been studied in the field of photocatalytic water splitting. Here, we present the direct decoration of Pt nanoparticles on CdSe tetrapod sidewalls synthesized by the continuous precursor injection (CPI) method. Pt-decorated CdSe tetrapods with different Pt nanoparticle size were synthesized and characterized by TEM, HR-TEM, XRD and HAADF-STEM. These tetrapods were employed as photocatalysts for the photocatalytic hydrogen generation reaction. The Pt-decorated CdSe tetrapods prepared with an extremely low amount of Pt precursor showed the highest photocatalytic H<sub>2</sub> generation efficiency, which is believed to be attributed to the size effect of Pt nanoparticles decorated on the CdSe tetrapod sidewalls.**

Colloidal hybrid nanomaterials, particularly metal-semiconductor hybrid nanocrystals, are of great interest due to the synergistic properties arising from different combinations of conducting and semiconducting structures within a single nanocrystal.<sup>1,2</sup> These hybrid nanomaterials show both metal and semiconductor properties with possible applications in the fields of self-assembly, electronic devices, photocatalysis, bioimaging, and so forth.<sup>3-10</sup> With their intrinsic properties of each metal and semiconductor, the heterostructured hybrid nanocrystals with various combinations and morphologies of metals and semiconductors have extensively been studied from fundamental mechanistic studies,<sup>2</sup> carrier dynamics<sup>11-</sup>

<sup>14</sup> to applications with a design for relevant use. Furthermore, complex heterostructures consisting of multicomponents of 2 or more semiconductors and metals were reported to precisely engineer morphologies as well as electronic properties of each component to achieve high-performance hybrid nanomaterials and devices.<sup>12, 14-15</sup>

Among many applications with the metal-semiconductor hybrid nanomaterials, the use of these heterostructured hybrid nanomaterials for photocatalysis has gained much attention due to increased interest in exploring new sources of renewable energy.<sup>34</sup> Novel metals such as Au or Pt were typically employed as cocatalysts when combined with semiconductor nanomaterials with light-absorbing properties to generate excitons. Proper bandgap engineering of these multicomponent hybrid nanocrystals enabled the increase in photocatalytic H<sub>2</sub> generation efficiencies by splitting water with electrons and holes generated.<sup>13</sup> More recently, many research groups have also shown the importance of the management of hole transfer rate that significantly affects the overall efficiency of photocatalytic H<sub>2</sub> generation reaction.<sup>12,16-18</sup> However, the electron transfer from semiconductor nanocrystals to metallic cocatalysts has still many remaining issues to be resolved. More specifically, platinum-incorporated cadmium chalcogenide semiconductor nanocrystals have been studied to improve the efficiency of photocatalytic H<sub>2</sub> generation reaction. Several research groups have already reported on the incorporation of Pt on cadmium chalcogenide nanocrystals with different synthetic mechanisms as well as with different morphologies. Tipping of Pt nanoparticles at the ends of CdSe or CdS nanorods and tetrapods has been introduced,<sup>10,19-20</sup> followed by the decoration of Pt nanoparticles by the photodeposition of Pt precursors under UV illumination.<sup>21-24</sup> These synthetic efforts enabled to design new hybrid nanocrystals and to study the carrier dynamics between Pt metal cocatalysts and CdSe or CdS semiconductor photocatalysts. Since metallic Pt nanoparticles act as reaction sites for the hydrogen evolution by combining with electrons generated from semiconductor nanocrystals, studies on the effect of Pt nanoparticles for the photocatalytic H<sub>2</sub> generation reaction have also been reported by many research groups. Feldmann and coworkers

<sup>a</sup>The National Creative Research Initiative Center for Intelligent Hybrids, Seoul National University, Seoul 08826, Republic of Korea.

<sup>b</sup>The World Class University (WCU) Program of Chemical Convergence for Energy & Environment, School of Chemical & Biological Engineering, Seoul National University, Seoul 08826, Republic of Korea.

<sup>c</sup>Department of Chemistry and Biochemistry, University of Arizona, Tucson, AZ, 85721 USA

<sup>d</sup>Chemistry Division, Los Alamos National Laboratory, Los Alamos, NM, 87545, USA

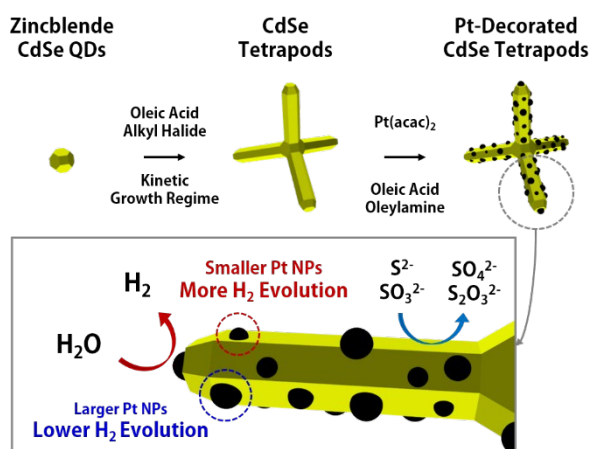
<sup>e</sup>Clean Energy Research Center, Korea Institute of Science and Technology (KIST), Seoul, 02792, Republic of Korea.

Electronic Supplementary Information (ESI) available: Synthetic and experimental details, and further characterizations are presented. See DOI: 10.1039/x0xx00000x

reported on the effect of the size of Pt clusters on photocatalytic H<sub>2</sub> evolution reaction. Pt clusters with a size of around 1 nm consisting of approximately 46 Pt atoms showed higher efficiency by properly matching the energy levels between Pt and CdS.<sup>25,26</sup> Xiong et al. also demonstrated with computational simulations that different size and shape of Pt clusters showed different adsorption characteristics on CdS nanocrystal surfaces.<sup>27</sup> They explained that the bonding interactions between metallic clusters and semiconductor nanocrystals affect the structural deformation as well as the modification of electronic structure, thus influencing the overall photocatalytic efficiency. Therefore, the surface properties of semiconductor nanocrystals combined with structural properties of metallic nanocrystals are important issues to be considered for the rational design of new metal-semiconductor hybrid photocatalysts.

A key criterion in the design of efficient photocatalysts lies in the reliable synthesis of semiconductor nanocrystals with different shape. A number of different synthetic methods have been reported for the shape control of semiconductor nanocrystals.<sup>28-30</sup> In general, controlling the surface energy of certain crystal facets by either using proper choices of strongly or weakly binding ligands, or controlling monomer concentration, is the commonly used approach. Alkylphosphonic acids were the typical ligands used to suppress the growth rate of specific crystal facets. However, due to the ease of scale-up along with economic issues, the use of other cheaper and easily-accessible ligands along with controlling other experimental parameters has been introduced. Our group has previously reported on the synthesis of well-defined CdSe tetrapods by using alkyl halides and also by keeping the arm growth stage within the kinetic growth regime. This synthetic method enabled us to easily scale-up the synthesis of tetrapods in gram scale with high morphological uniformity and shape selectivity.<sup>31</sup> As a result, each of these semiconductor nanocrystals prepared with different synthetic schemes has resulted in different surface chemistry and topography, which then need to be considered for further rational design of metal-semiconductor hybrid nanocrystals.

Herein, we report on the direct deposition of Pt nanoparticles on CdSe tetrapod sidewalls and their photocatalytic H<sub>2</sub> generation behaviour. CdSe tetrapods synthesized by the continuous precursor injection (CPI) approach, previously reported by our group,<sup>31</sup> showed



**Scheme 1** Schematic illustration of the overall synthesis of Pt-decorated CdSe tetrapods and their photocatalytic hydrogen generation application.

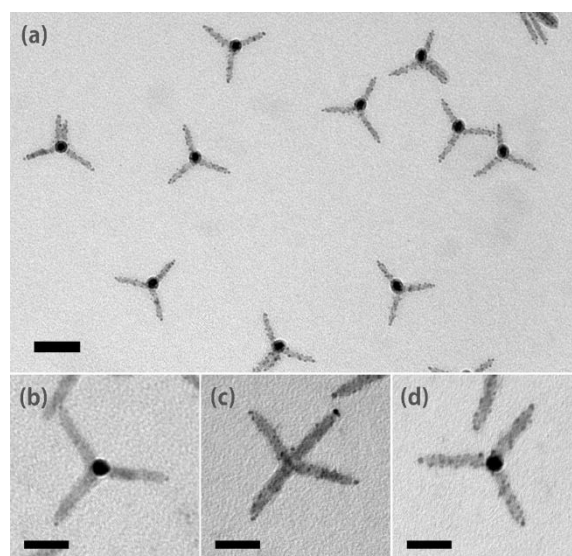


**Fig. 1** TEM images of Pt-decorated CdSe tetrapods with (a) low magnification (scalebar = 50 nm) and (b-d) the effect of controlled amount of Pt precursors of 1 mg, 15 mg and 25 mg relative to 25 mg of CdSe tetrapods (scalebar = 25 nm).

the uniform decoration of Pt nanoparticles on the entire surface of CdSe tetrapod arms (Scheme 1). We also noted that the controlled amount of Pt precursors has resulted in the different size of Pt nanoparticles. These Pt-decorated CdSe tetrapods were then used for the photocatalytic H<sub>2</sub> generation due to water splitting reaction. Among Pt-decorated CdSe tetrapods prepared with different ratios of the amount of Pt precursors with respect to a fixed amount of CdSe tetrapods, Pt nanoclusters with the smallest size formed on the CdSe tetrapod arms showed the highest photocatalytic H<sub>2</sub> generation efficiency. This result explains that different surface chemical states of CdSe semiconductor nanocrystals lead to different mechanism for novel metal nanoparticles to nucleate and grow, suggesting new types of semiconductor nanocrystals and eventually new classes of metal-semiconductor hybrid nanocrystals for various applications.

Figure 1 shows the transmission electron microscopy images of Pt-decorated CdSe tetrapods with different size of Pt nanoparticles. First, the CdSe tetrapods were synthesized by using zincblende CdSe quantum dots as seeds, followed by using oleic acid and alkyl halides as mixed ligands for the growth of wurtzite CdSe tetrapod arms. Specific amount of alkyl halides, in the representative synthetic procedure (for the present case, cetyltrimethylammonium bromide) were adopted as alkyl halide ligands), was necessary to maintain the growth of wurtzite CdSe arms within the kinetic growth regime.<sup>31</sup> After several purification steps, as-synthesized CdSe tetrapods were used for the decoration of Pt nanoparticles with the procedure previously reported.<sup>10</sup> Interestingly, we noted that Pt nanoparticles were nucleated and grown throughout the entire region of CdSe tetrapod arms, and the control of the amount of Pt precursors resulted in Pt nanoparticles of different size formed on the surface of CdSe tetrapod arms. Typically, novel metal nanoparticles such as Au and Pt are known to nucleate at the surface sites of semiconductor nanocrystals of high energy, which are typically the termini of nanocrystals with anisotropic shapes, or lattice defects generated during the synthesis. However, in the present case, uniform distribution of Pt nanoparticles decorated on the entire surface of

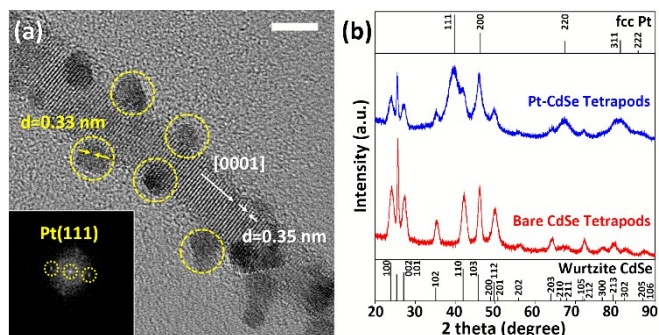


**Fig. 2** (a) A HR-TEM image of Pt-decorated CdSe tetrapods with a FFT pattern of fcc Pt nanoparticles (inset) (scale bar = 5 nm). (b) Powder XRD spectra of bare CdSe tetrapods and Pt-decorated CdSe tetrapods.

CdSe tetrapod arms was observed. The increase in the amount of Pt precursors resulted in the formation of larger Pt nanoparticles, yet maintaining the areal number density of Pt nanoparticles formed at the surface of CdSe tetrapods. Further ICP-AES analysis also confirmed the increase in Pt concentration on the tetrapod arms with the increase in the amount of Pt precursors added (Table S1). From normal TEM images with the samples prepared with different amounts of Pt precursors, it is hard to distinguish the presence of Pt nanoparticles with extremely small size. However, the uniform decoration of Pt nanoparticles on the tetrapod arms was confirmed and will be explained later in more detail. We assume that when compared with previously reported methods to prepare CdSe nanocrystals with anisotropic shape, since a fixed amount of alkyl halides was introduced to the system during the arm growth, this procedure might lead to the surface chemical states different from other CdSe nanorods or tetrapods previously reported. We believe that the introduction of alkyl halides, which is crucial for the synthesis of CdSe tetrapods, enables the decoration of Pt nanoparticles throughout the entire surface of CdSe tetrapods due to Cd-halide ligand-free sites on the surface sidewalls of wurtzite CdSe tetrapod arms.<sup>31</sup> Further detailed mechanistic studies along with structural analysis are currently under progress.

Structural analyses of Pt-decorated CdSe tetrapods were performed by high-resolution transmission electron microscopy (HR-TEM) and powder X-ray diffraction (XRD) measurement (Figure 2). From HR-TEM images, the crystal lattice structure of wurtzite CdSe arms as well as Pt nanoparticles in face-centered cubic lattice was confirmed by the d-spacing values as well as the fast Fourier transform (FFT) pattern. From XRD, when no Pt nanoparticles were incorporated onto CdSe tetrapods, distinct peaks only from the wurtzite CdSe tetrapod arms were observed, referenced to JCPDS 08-0409. After the decoration of Pt nanoparticles on the CdSe tetrapods, peaks from the fcc Pt nanoparticles were identified, confirming the presence of Pt nanoparticles decorated on the CdSe tetrapods, referenced to JCPDS 04-0802. The existence of Pt clusters on the CdSe tetrapod surface is further confirmed by XPS analysis (Figure S4).

In figure 3, from the HAADF-STEM images, the bright region corresponds to Pt nanoparticles with higher electron density when compared with semiconducting CdSe tetrapods. As mentioned earlier, normal TEM could not clearly confirm the existence of Pt nanoparticles formed on the CdSe tetrapods when an extremely low amount of Pt precursors was introduced. But, by the HAADF-STEM

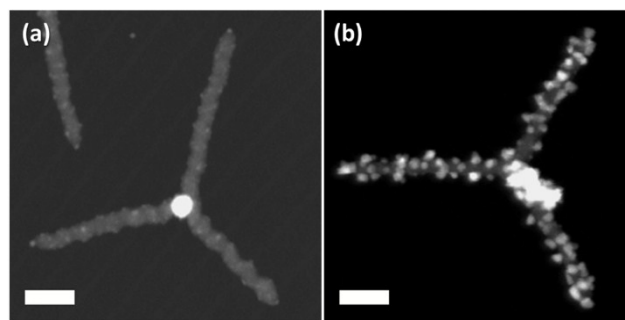


**Fig. 3** HAADF-STEM images of Pt-decorated CdSe tetrapods with (a) 1 mg and (b) 25 mg amount of Pt precursors (scale bar = 20 nm).

images, the existence of Pt nanoparticles even with very small size ( $\sim 1$  nm) was observed (Figure 3(a)). Moreover, control experiments for the growth of second metal and previous reports by Pyun and Cho et al. also support this argument. During the Pt-tipping reaction with CdSe@CdS nanorods, when the reaction time for Pt to nucleate and grow was kinetically suppressed, only one Pt tip or no tip was observed by normal TEM, called the “activated” CdSe@CdS nanorods.<sup>5,6,32</sup> Followed by the growth of second metal nanoparticles, which in this case were cobalt, the existence of Pt nanoparticles was indirectly confirmed since cobalt nanoparticles were only formed epitaxially when Pt tips were first introduced to the ends of CdSe@CdS nanorods.<sup>33</sup> Control experiment was performed by growing cobalt nanoparticles in the presence of bare CdSe tetrapods synthesized by the CPI approach and Pt-decorated CdSe tetrapods with an extremely low amount of Pt precursors (Figure S2). When no Pt nanoparticles were introduced to the CdSe tetrapods, no cobalt nanoparticles were formed at the surface of CdSe tetrapods. Although an extremely low amount of Pt precursors was introduced, the conformal decoration of cobalt nanoparticles on the Pt-decorated CdSe tetrapods was also observed. This result confirms the existence of Pt nanoparticles on the Pt-decorated CdSe tetrapods, but with very small in size.

As-synthesized Pt-decorated CdSe tetrapods with different amount of Pt precursors were then used to examine the photocatalytic  $H_2$  generation efficiency. A series of Pt-decorated CdSe tetrapods were prepared by controlling the amount of Pt precursors and used as photocatalysts. The amount of CdSe tetrapods used for the decoration of Pt nanoparticles was fixed at 25 mg, whereas the amount of Pt precursors was varied from 1 to 25 mg. Simply by the ligand exchange of Pt-decorated CdSe tetrapods with mercaptoundecanoic acids, the Pt-decorated CdSe tetrapods were well-dispersed in hydrophilic solvents (i.e., water) without any structural transformation or aggregation. The amount of Pt-CdSe hybrid tetrapod photocatalysts was fixed at 2.5 mg and dispersed in 0.35 M  $Na_2SO_3/0.25$  M  $Na_2S$  aqueous solution under the 1 SUN illumination condition. Figure 4(a) shows the amount of  $H_2$  evolved by the Pt-decorated CdSe tetrapods with different amount of Pt precursors plotted against time for a period of 30 min. All the Pt-decorated CdSe tetrapods tested in the present study showed the photocatalytic  $H_2$  generation behaviour with relatively the linear increase with time (Figure S4). Interestingly, when the extremely low amount of Pt precursors was introduced into the CdSe tetrapods, much higher amount of  $H_2$  was generated when compared with other tetrapods with larger size of Pt nanoparticles decorated. When

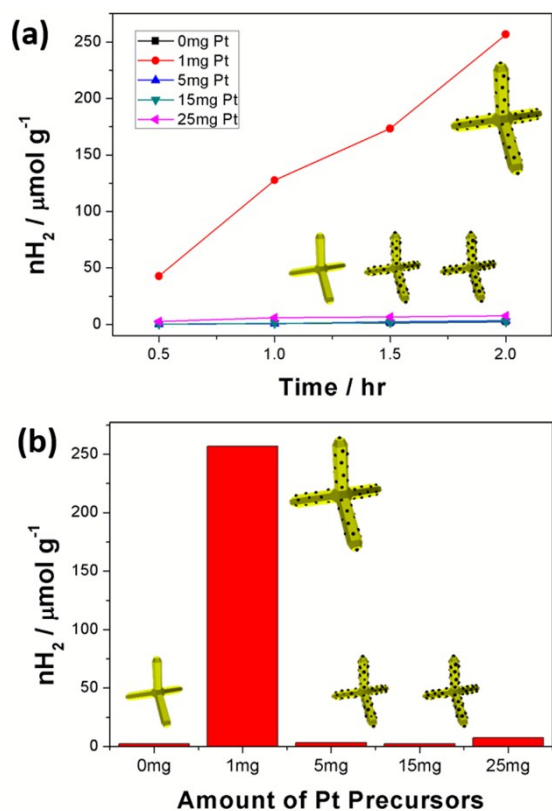


**Fig. 4** Photocatalytic hydrogen generation from the Pt-decorated CdSe tetrapods with different size of Pt nanoparticles (a) as a function of time and (b) as the amount of Pt precursors used for the decoration.

1 mg of Pt precursors was used for the decoration of Pt nanoparticles on the surfaces of the CdSe tetrapods, the average size of the Pt nanoparticles was hard to measure, but approximately less than 1.5 nm, which is the smallest size possible to identify with our TEM. The increase in the amount of Pt precursors resulted in Pt nanoparticles with distributions of particle size, implying that both small (less than 1.5 nm) and larger (~ 2.5 nm) Pt nanoparticles coexist. The result that the CdSe tetrapods containing less than 1.5 nm Pt nanoparticles show higher efficiency could be explained from the literature, which the Pt cluster size significantly affects the photocatalytic activity of metal-semiconductor hybrid nanomaterials.<sup>25-27</sup> The LUMO of Pt nanoparticles should be located between the conduction band of semiconductors and the H<sup>+</sup>/H<sub>2</sub> reduction potential in order to promote the electron transfer. In our system, the controlled amount of Pt precursors resulted in the different size of Pt nanoparticles formed on the surfaces of CdSe tetrapods. Meanwhile, the number density for the nucleation sites for Pt formation on the CdSe tetrapods is, more or less, fixed by the amount of CTAB ligands in the mixed ligands.<sup>31</sup> Therefore, the formation of Pt nanoparticles of different size simply by controlling the amount of Pt precursors, with a fixed number density of Pt nanoparticles formed on the surface of CdSe tetrapods, was observed. This is believed to change the LUMO energy level of Pt nanoparticles and when larger Pt nanoparticles, of which the LUMO energy level is misplaced for the photocatalytic H<sub>2</sub> generation, showed significantly low photocatalytic activity.

## Conclusions

We have successfully synthesized the Pt-decorated CdSe tetrapods with controlled Pt nanoparticle size. The CdSe tetrapods prepared in the presence of alkyl halide ligands led to the direct incorporation of Pt nanoparticles without post treatment. These hybrid tetrapods had a fixed number density for nucleation sites, enabling to assess the size effect of Pt nanoparticles formed uniformly on the CdSe tetrapods on the photocatalytic activity of H<sub>2</sub> generation reaction. An extremely low amount of Pt precursors employed for Pt nanoparticle synthesis resulted in the uniform incorporation of Pt nanoparticles with very small size, which in turn, well matches with the energy levels of CdSe semiconductor arms and the H<sup>+</sup>/H<sub>2</sub> reduction potential, showed the highest photocatalytic efficiency. The result shown in the present study opens another avenue for the rational design of new types of metal-semiconductor hybrid nanomaterials to further increase the photoconversion efficiency in the photocatalytic water splitting reaction.

## Acknowledgements

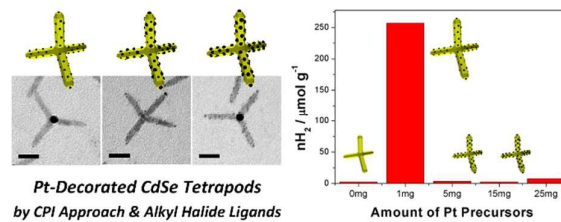
K.C. acknowledges the financial support from the National Research Foundation of Korea (NRF) for the National Creative Research Initiative Center for Intelligent Hybrids (No. 2010-0018290). Both K.C. and J.P. acknowledge the World Class University Program of Chemical Convergence for Energy & Environment (R31-10013). J.P. acknowledges the financial support from the U.S. Department of Energy, Office of Basic Energy Sciences, Solar Photochemistry Program (DE-FG03-02ER15753) and the National Science Foundation (DMR-130792).

## Notes and references

- 1 T. Mokari, E. Rothenberg, I. Popov, R. Costi and U. Banin, *Science*, 2004, **304**, 1787.
- 2 T. Mokari, C. G. Sztrum, A. Salant, E. Rabani and U. Banin, *Nat. Mater.*, 2005, **4**, 855.
- 3 U. Banin, Y. Ben-Shahar and K. Vinokurov, *Chem. Mater.*, 2014, **26**, 97.
- 4 A. Salant, E. Amitay-Sadovsky and U. Banin, *J. Am. Chem. Soc.*, 2006, **128**, 10006.
- 5 L. J. Hill, N. E. Richey, Y. Sung, P. T. Dirlam, J. J. Griebel, E. Lavoie-Higgins, I. -B. Shim, N. Pinna, M. -G. Willinger, W. Vogel, J. J. Benkoski, K. Char and J. Pyun, *ACS Nano*, 2014, **8**, 3272.
- 6 L. J. Hill, N. Pinna, K. Char and J. Pyun, *Prog. Polym. Sci.*, 2015, **40**, 85.
- 7 D. Kim, W. D. Kim, M. S. Kang, S. -H. Kim and D. C. Lee, *Nano Lett.*, 2015, **15**, 714.
- 8 A. Figuerola, I. R. Franchini, A. Fiore, R. Mastria, A. Falqui, Bertonni, S. Bals, G. V. Tendeloo, S. Kudera, R. Cingolani and I. Mann, *Adv. Mater.*, 2009, **21**, 550.
- 9 R. Costi, A. E. Saunders, E. Elmalem, A. Salant and U. Banin, *Nano Lett.*, 2008, **8**, 637.
- 10 L. Amirav and A. P. Alivisatos, *J. Phys. Chem. Lett.*, 2010, **1**, 1051.
- 11 K. Wu, H. Zhu and T. Lian, *Acc. Chem. Res.*, 2015, **48**, 851.

- 12 K. P. Acharya, R. S. Khnayzer, T. O'Connor, G. Diederich, M. Kirsanova, A. Klinkova, D. Roth, E. Kinder, M. Imboden and M. Zamkov, *Nano Lett.*, 2011, **11**, 2919.
- 13 M. J. Berr, A. Vaneski, C. Mauser, S. Fischbach, A. S. Sussha, A. K. Rogach, F. Jäckel and J. Feldmann, *Small*, 2012, **8**, 291.
- 14 T. O'Connor, M. S. Panov, A. Mereshchenko, A. N. Tarnovsky, R. Lorek, D. Perera, G. Diederich, S. Lambricht, P. Moroz and M. Zamkov, *Nano Lett.*, 2012, **6**, 8156.
- 15 N. Oh, S. Nam, Y. Zhai, K. Deshpande, P. Trefonas and M. Shim, *Nat. Commun.*, 2014, **5**, 3642.
- 16 M. J. Berr, P. Wagner, S. Fischbach, A. Vaneski, J. Schneider, A. S. Sussha, A. L. Rogach, F. Jäckel and J. Feldmann, *Appl. Phys. Lett.*, 2012, **100**, 223903.
- 17 K. Wu, Z. Chen, H. Lv, H. Zhu, C. L. Hill and T. Lian, *J. Am. Chem. Soc.*, 2014, **136**, 7708.
- 18 T. Simon, N. Bouchonville, M. J. Berr, A. Vaneski, A. Adrović, D. Volbers, R. Wyrwich, M. Döblinger, S. A. Sussha, A. L. Rogach, F. Jäckel, J. K. Stolarczyk and J. Feldmann, *Nat. Mater.*, 2014, **13**, 1013.
- 19 S. E. Habas, P. Yang and T. Mokari, *J. Am. Chem. Soc.*, 2008, **130**, 3294.
- 20 J. U. Bang, S. J. Lee, J. S. Jang, W. Choi and H. Song, *J. Phys. Chem. Lett.*, 2012, **3**, 3781.
- 21 G. Dukovic, M. G. Merkle, J. H. Nelson, S. M. Hughes and A. P. Alivisatos, *Adv. Mater.*, 2008, **20**, 4306.
- 22 M. Berr, A. Vaneski, A. S. Sussha, J. Rodríguez-Fernández, M. Döblinger, F. Jäckel, A. L. Rogach and J. Feldmann, *Appl. Phys. Lett.*, 2010, **97**, 093108.
- 23 J. Lian, Y. Xu, M. Lin and Y. Chan, *J. Am. Chem. Soc.*, 2012, **134**, 8754.
- 24 E. Conca, M. Aresti, M. Saba, M. F. Casula, F. Quochi, G. Mula, D. Loche, M. R. Kim, L. Manna, A. Corrias, A. Mura and G. Bongiovanni, *Nanoscale*, 2014, **6**, 2238.
- 25 M. J. Berr, F. F. Schweinberger, M. Döblinger, K. E. Sanwald, C. Wolff, J. Breimeier, A. S. Crampton, C. J. Ridge, M. Tschurl, U. Heiz, F. Jäckel and J. Feldmann, *Nano Lett.*, 2012, **12**, 5903.
- 26 F. F. Schweinberger, M. J. Berr, M. Döblinger, C. Wolff, K. E. Sanwald, A. S. Crampton, C. J. Ridge, F. Jäckel, J. Feldmann, M. Tschurl and U. Heiz, *J. Am. Chem. Soc.*, 2013, **135**, 13262.
- 27 S. Xiong, E. B. Isaacs and Y. Li, *J. Phys. Chem. C.*, 2015, **119**, 4834.
- 28 D. V. Talapin, J. H. Nelson, E. V. Shevchenko, S. Aloni, B. Sadtler and A. P. Alivisatos, *Nano Lett.*, 2007, **7**, 2951.
- 29 S. Asokan, K. M. Krueger, V. L. Colvin and M. S. Wong, *Small*, 2007, **3**, 1164.
- 30 L. Liu, Z. Zhuang, T. Xie, Y. -G. Wang, J. Li, Q. Peng and Y. Li, *J. Am. Chem. Soc.*, 2009, **131**, 16423.
- 31 J. Lim, W. K. Bae, K. U. Park, L. zur Borg, R. Zentel, S. Lee and K. Char, *Chem. Mater.*, 2012, **25**, 1443.
- 32 L. J. Hill, M. M. Bull, Y. Sung, A. G. Simmonds, P. T. Dirlam, N. E. Richey, S. E. DeRosa, I. -B. Shim, D. Guin, P. J. Costanzo, N. Pinna, M. -G. Willinger, W. Vogel, K. Char and J. Pyun, *ACS Nano*, 2012, **6**, 8632.
- 33 L. J. Hill, N. E. Richey, Y. Sung, P. T. Dirlam, J. J. Griebel, I. -B. Shim, N. Pinna, M. -G. Willinger, W. Vogel, K. Char and J. Pyun, *CrystEngComm.*, 2014, **16**, 9461.
- 34 J. Ran, J. Yu and M. Jaroniec, *Green Chem.*, 2011, **13**, 2708.
- 35 J. Yu, Y. Yu and B. Cheng, *RSC Adv.*, 2012, **2**, 11829.
- 36 Y. Xu and R. Xu, *Appl. Surf. Sci.*, 2015, **351**, 779.
- 37 H. Ahmad, S. K. Kamarudin, L. J. Minggu and M. Kassim, *Renew. Sustain. Energ. Rev.*, 2015, **43**, 599.
- 38 V. Preethi and S. Kanmani, *Mat. Sci. Semicon. Proc.*, 2013, **16**, 561.
- 39 X. Li, J. Yu, J. Low, Y. Fang, J. Xiao and X. Chen, *J. Mater. Chem. A*, 2015, **3**, 2485.

## Table of Contents



*Direct Decoration of Pt Nanoparticles onto CdSe Tetrapods with Controlled Size and Their Photocatalytic H<sub>2</sub> Generation Efficiency.*